

Intermetallic Hydrides as Zintl Phases: A_3TtH_2 Compounds ($A = Ca, Yb; Tt = Sn, Pb$) and Their Structural Relationship to the Corresponding Oxides

Baoquan Huang and John D. Corbett*

Ames Laboratory—DOE¹ and Department of Chemistry, Iowa State University, Ames, Iowa 50011

Received March 13, 1997[⊗]

Shiny crystals of the isotopic title compounds are obtained in high yield from suitable proportions of AH_2 , metal A , and Sn or Pb in welded Ta containers slowly cooled from 1100 °C. These were characterized by single-crystal X-ray diffraction for Ca_3SnH_2 and Ca_3PbH_2 (orthorhombic, $Cmcm$ (No. 63), $Z = 4$, $a = 8.866(1)$, $8.937(1)$ Å, $b = 11.371(2)$, $11.470(2)$ Å, $c = 5.220(1)$, $5.2551(7)$ Å, respectively). The structure contains distorted hcp layers of Ca_3Tt between which hydrogen occupies all tetrahedral voids formed by Ca atoms. These tetrahedra share three edges to form double chains along the c axis that are separated by Tt atoms. Both calcium compounds are diamagnetic semiconductors, and the family can all be formulated in terms of oxidation states as Zintl phases $(A^{+2})_3Tt^{-4}(H^-)_2$. Their structure may be derived from the hexagonal version of the cubic perovskitic Ca_3SnO by distortions that split the octahedral site in the oxide into edge-sharing tetrahedral pairs.

Introduction

Hydrogen in transition metals and their intermetallic compounds has been extensively studied with regard to potential applications for the storage of hydrogen.^{2,3} The hydrogen atoms in these materials are generally believed to have acquired electrons from the conduction band, i.e., to be hydrides, but the compounds are often nonstoichiometric and metallic. The second class of well known solid state materials is complex transition-metal hydrides that contain complex anions MH_x^{n-} in which hydrogen is covalently bonded to a transition element.^{4,5} These usually show semiconducting or insulating properties.

Hydrogen as an interstitial or anionic component in phases formed between the active metals and the later main-group (p-block) elements has been relatively ignored. This is particularly serious for the alkaline-earth metals (Ae) because their common contamination with hydrogen has often gone unrecognized, and hydrogen of course would generally not be discerned during an X-ray diffraction study. Synthetic precautions in control reactions with and without hydrogen have proven the most useful diagnoses. Thus, some so-called “unusual” compounds, which have often been difficult to secure in high yield and contradict Zintl (closed shell) valence rules,⁶ have been shown to be hydrogen-stabilized phases. Recently, we have learned how to quantitatively synthesize phases in the series of Ae_5Pn_3H ($Pn = As, Sb, Bi$) (“ Yb_5Sb_3 ”-type),^{7,8} Ae_5Tt_3H ($Tt = Si, Ge, Sn, Pb$) and $Sr_5Tl_3H^9$ (stuffed Cr_5B_3 or La_5Pb_3O -type¹⁰),

and $Ba_5Ga_6H_2$.¹¹ Here we present the synthesis and characterization of a new family of hydrogen-stabilized Zintl compounds: Ca_3SnH_2 , Ca_3PbH_2 , Yb_3SnH_2 , and Yb_3PbH_2 . The single type of hydrogen atom in the first compound was located and refined by X-ray diffraction methods. These compounds were investigated because they represent the hydride analogues of well-known oxygen contamination products typified by cubic Ca_3SnO .¹²

Experimental Section

Syntheses. Sublimed calcium metal (APL Engineered Materials, Urbana, IL, 99.99 %), ytterbium (Ames Lab, 4–9’s total), and their binary and ternary hydrides are sensitive to air and moisture, and they were therefore handled only in He- or N_2 -filled gloveboxes. The calcium as received contained hydrogen, perhaps ~5 at. %. Calcium hydride was prepared from calcium metal and 600 Torr hydrogen (Matheson, 99.999 %) at 800 °C for 12 h as described elsewhere.^{8,9} The synthesis of YbH_2 required a higher temperature, 900 °C. Their Guinier X-ray patterns indicated only the nominal dihydrides were present. The Sn and Pb utilized were Baker’s Analyzed and Aesar, respectively, both labeled as 5–9’s metal purity.

CaH_2 , Ca , and Sn or Pb in various ratios (Table 1) were welded in Ta containers under Ar , which were then jacketed in evacuated, flamed and sealed SiO_2 tubing to protect them from air. The contents were melted at 1100 °C, kept at that temperature for 4 h, and then slowly cooled at a rate of 20 °C h^{-1} . When necessary, pure Ca in another Ta container within the same SiO_2 jacket was used to absorb any hydrogen excess. The Yb_3TtH_2 phases (Table 1) synthesized in a parallel manner were obtained in 50–75 % yields along with Yb_2Tt and YbH_2 . Further reaction of these in the presence of 300 Torr H_2 increased the yields of 85 and 90 %. The products were silvery and, with Ca , sensitive to air. Guinier patterns were obtained from ground samples mounted between pieces of cellophane tape with the aid of an Enraf-Nonius Guinier Camera, $Cu K\alpha$ radiation ($\lambda = 1.54056$ Å) and NIST silicon ($a = 5.43088$ Å) as an internal standard. Table 2 gives the cell parameters refined from indexed lines and their 2θ values determined with the aid of a nonlinear fit to the positions of the Si lines.

Structural Studies. The relatively simple pattern of the first Ca_3SnH_2 sample (Table 1) was well indexed to a C -centered orthorhombic

[⊗] Abstract published in *Advance ACS Abstracts*, July 1, 1997.

- (1) This research was supported by the Office of the Basic Energy Sciences, Materials Sciences Division, U.S. Department of Energy. The Ames Laboratory is operated by Iowa State University under Contract No. W-7405-Eng.82.
- (2) Hydrogen in Metals I, II. *Topics in Applied Physics*; Alefeld, G., Volkl, J., Eds.; Springer: Berlin, 1978; Vols. 28, 29.
- (3) Hydrogen in Intermetallic Compounds I, II. *Topics in Applied Physics*; Schlapbach, L., Ed.; Springer: Berlin, 1988, 1992; Vols. 63, 67.
- (4) Bronger, W. *Angew. Chem., Int. Ed. Engl.* **1991**, *30*, 759.
- (5) Yvon, K. In *Encyclopedia of Inorganic Chemistry*; King, R. B., Ed.; Wiley: New York, 1994; Vol. 3, p 1401.
- (6) Kauzlarich, S. Ed. *Chemistry, Structure and Bonding of Zintl Phases and Ions*; VCH Publishers: Boca Raton, FL, 1996.
- (7) Leon-Escamilla, E. A.; Corbett, J. D. *J. Alloys Compd.* **1994**, *206*, L15.
- (8) Leon-Escamilla, E. A.; Corbett, J. D. *J. Alloys Compd.*, in press.
- (9) Leon-Escamilla, E. A. Ph.D. Dissertation, Iowa State University, 1996.

(10) Guloy, A.; Corbett, J. D. *Z. Anorg. Allg. Chem.* **1992**, *616*, 61.

(11) Henning, R. W.; Leon-Escamilla, E. A.; Zhao, J.-T.; Corbett, J. D. *Inorg. Chem.* **1997**, *36*, 1282.

(12) Widera, A.; Schafer, H. *Mater. Res. Bull.* **1980**, *15*, 1805.

Table 1. Synthesis Conditions and Products

loaded compn	method ^a	principal phase, yield ^b	second phase, yield ^{b,c}
Ca ₃ SnH ₆	I	Ca ₃ SnH ₂ , >95%	none ^c
Ca ₃ SnH ₄	I	Ca ₃ SnH ₂ , >95%	none
Ca ₃ SnH ₃	I	Ca ₃ SnH ₂ , >95%	none
Ca ₃ SnH ₂	I	Ca ₃ SnH ₂ , 90%	Ca ₂ Sn, 10%
Ca ₃ Sn	II	Ca ₂ Sn, 85%	Ca
Ca ₃ PbH ₆	I	Ca ₃ PbH ₂ , >95%	none
Ca ₃ PbH ₄	I	Ca ₃ PbH ₂ , >95%	none
Ca ₃ PbH ₃	I	Ca ₃ PbH ₂ , >95%	none
Ca ₃ PbH ₂	I	Ca ₃ PbH ₂ , 90%	Ca ₂ Pb, 10%
Ca ₃ Pb	II	Ca ₂ Pb, 85%	Ca
Yb ₃ SnH ₂	III	Yb ₃ SnH ₂ , 85%	Yb ₂ Sn, 10 %; YbH ₂ , 5 %
Yb ₃ PbH ₂	III	Yb ₃ PbH ₂ , 90%	Yb ₂ Pb, 7 %; YbH ₂ , 3 %

^a I: Ta container enveloped by a sealed silica jacket. The Ca was used as received, and Ca in a second Ta container absorbed the excess hydrogen. II: Welded Ta container under dynamic high vacuum. III: As with I, except that the products were ground and reacted with 300 Torr H₂ at 1100 °C for 4 h. ^b Visually estimated from X-ray Guinier films in terms of equivalent scattering power. ^c Estimated detection limit is <5 mol %.

Table 2. Lattice Dimensions of A₃TtH₂ Phases (Cmcm) (Å, Å³)^a

	<i>a</i>	<i>b</i>	<i>c</i>	<i>V</i>
Ca ₃ SnH ₂	8.866(1)	11.371(2)	5.220(1)	526.3(3)
Ca ₃ PbH ₂	8.937(1)	11.470(2)	5.2251(7)	538.7(3)
Yb ₃ SnH ₂	8.833(3)	11.296(3)	5.234(2)	522.2(5)
Yb ₃ PbH ₂	8.901(3)	11.399(3)	5.254(2)	533.1(5)

^a From Guinier powder diffraction with Si as an internal standard, λ = 1.540 562 Å, 22 °C.

cell by TREOR.¹³ A few crystals were sealed in glass capillaries and checked for singularity by oscillation film techniques. An octant of intensity data was collected from one on a Rigaku AFC-6R rotating anode diffractometer (Mo Kα radiation, graphite monochromator) at room temperature with an ω-2θ scan mode for 2θ up to 50°. Assignment of space group Cmcm (No. 63) was made on the basis of the systematic absences and a statistical analysis of intensity distribution, and this choice was supported by the subsequent successful refinement. Metal atomic positions were established by direct methods via SHELXS.¹⁴ Substantial absorption effects for the platelike crystal were corrected empirically according to the average of three ψ-scan curves at different θ values and later, after isotropic refinement, by DIFABS.¹⁵ Preliminary anisotropic refinement of the metal positions in Ca₃SnH₂ with the TEXSAN package¹⁶ on a VAX station converged at the residuals R(F) = 1.9 %, R_w = 2.8 %. Hydrogen positions were located on the difference Fourier map (peak height: 1.1 e/Å³) reproduced in Figure 1. (There are no further cavities in the structure suitable for hydrogen.) Preliminary refinement gave a hydrogen occupancy factor of 1.12(6) (U fixed), and this was thereafter fixed at unity for the final refinements. The final refinements, including the atomic position and isotropic thermal amplitude parameters of hydrogen, converged at R(F) = 1.5 %, R_w = 1.9 % (283 independent reflections, 16 variables). The largest residual peaks in the final Fourier map were 0.56 e/Å³ at (0.0, 0.383, 1/4) in the vicinity of Ca2 atom (~1.79 Å) and -0.69 e/Å³ at (0.292, 0.386, 1/4), respectively.

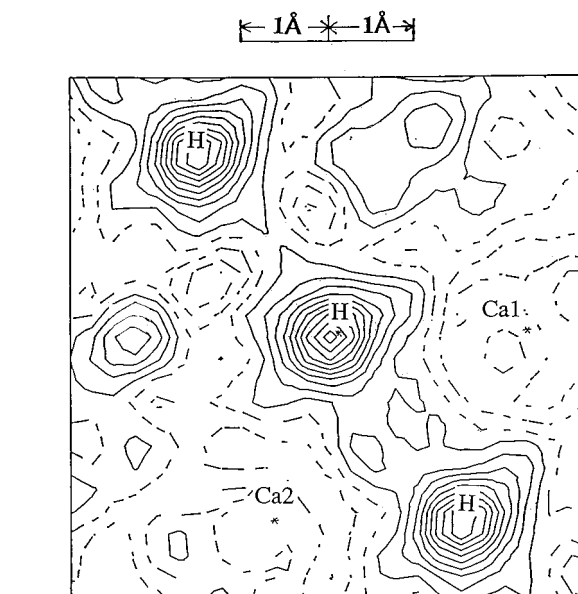
The structural refinement for Ca₃PbH₂ started with the atomic parameters for the stannide, and this proceeded with fixed position and displacement amplitude for hydrogen from the first study to convergence at R(F) = 2.3 %, R_w = 2.5 % (271 reflections > 3σ_I, 14 variables, μ = 342 cm⁻¹). Some data collection and refinement parameters are summarized in Table 3. Additional collection and refinement information and the anisotropic displacement parameters are available as

(13) Werner, P. E.; Eriksson, L.; Westdahl, M. *J. Appl. Crystallogr.* **1985**, *18*, 367.

(14) Sheldrick, G. M. SHELXS-86, Universität Göttingen, Germany, 1986.

(15) Walker, N.; Stuart, D. *Acta Crystallogr.* **1983**, *A39*, 158.

(16) TEXSAN, Version 6.0, Molecular Structure Corp., The Woodlands, TX, 1990.

**Figure 1.** X-ray difference electron density map for Ca₃SnH₂ as phased by Ca and Sn, revealing the H atom locations (0.1 e/Å³ contour intervals).**Table 3.** Crystallographic Data for Ca₃SnH₂ and Ca₃PbH₂

formula	Ca ₃ SnH ₂	Ca ₃ PbH ₂
fw	240.95	329.4
space group, Z ^a	Cmcm (No. 63), 4	Cmcm (No. 63), 4
d _{calc} (g/cm ³)	3.041	4.062
R, R _w ^b	0.015, 0.019	0.023, 0.025

^a Lattice parameters in Table 2. ^b R = Σ||F_o - |F_c||/Σ|F_o|, R_w = [Σw(|F_o - |F_c||)²/ΣwF_o²]^{1/2}, w = σ_F⁻².

Supporting Information, and these plus the structure factor data are also available from J.D.C.

Physical Property Measurements. The electrical resistivities of the two calcium compounds were measured with an electrodeless high-frequency "Q" method. The samples were ground, and a fraction with an average particle diameter of 340 μm was separated and mixed with chromatographic Al₂O₃ in order to reduce contact between the sample particles. The mixture was loaded into a glass ampule and sealed under vacuum. The Q measurements were made over 100–295 K with readings every 15°. The magnetic susceptibilities of the same compounds were measured at 3 T over the range 6–300 K on a Quantum Design MPMS SQUID magnetometer. The special container¹⁷ was constructed of fused-silica tubing such that a 50-mg sample was held between the faces of two fixed silica rods. The assembly was evacuated, backfilled with He, and sealed. Data were corrected for the container and for core diamagnetism.

Results and Discussion

Syntheses. Ca₃SnH₂ and Ca₃PbH₂ are obtained quantitatively from reactions of CaH₂ with Ca plus Sn or Pb at 1100 °C followed by slow cooling (see Table 1). Reactions in the absence of hydrogen give only a mixture of the binary intermetallics Ca₂Sn or Ca₂Pb (Co₂Si-type¹⁸) and Ca. The behavior of Yb is quite parallel. Comparable reactions demonstrated that isotypic compounds are not formed in the presence of hydrogen by Ca plus Si or Ge or with Sr or Ba plus Sn or Pb, only mixtures of other known phases.

Crystal Structure. Structures of the isotypic Ca₃SnH₂ and Ca₃PbH₂ were both refined. The final atomic coordinates, the isotropic-equivalent temperature factors, and their estimated standard deviations are listed in Table 4, and important distances,

(17) Guloy, A. M.; Corbett, J. D. *Inorg. Chem.* **1996**, *35*, 4670.

(18) Eckerlin, P.; Leicht, E.; Wolfel, E. *Z. Anorg. Allg. Chem.* **1961**, *307*, 145.

Table 4. Positional and Isotropic-Equivalent Displacement Parameters for Ca_3TtH_2 (Tt = Sn, Pb)

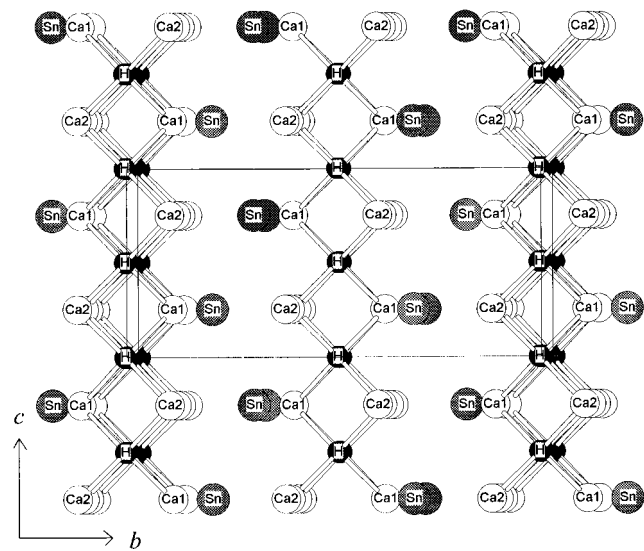
atom	Wyckoff type	x	y	z	$U_{\text{iso}} (\times 10^2)$, \AA^2 ^a
Ca_3SnH_2					
Ca1	4c $m2m$	0	0.1105(1)	$1/4$	1.38(5)
Ca2	8g m	0.2021(1)	0.38853(7)	$1/4$	1.81(4)
Sn	4c $m2m$	0	0.69299(3)	$1/4$	1.37(2)
H	8e 2	0.149(5)	0	0	1.8(9)
Ca_3PbH_2					
Ca1	4c $m2m$	0	0.1099(2)	$1/4$	1.4(1)
Ca2	8g m	0.2026(2)	0.3884(2)	$1/4$	1.32(8)
Pb	4c $m2m$	0	0.69275(4)	$1/4$	0.98(2)
H ^b	8e 2	0.149	0	0	1.8

^a $U_{\text{iso}} = (1/3)\sum_i\sum_j U_{ij}a_i^*a_j^*\vec{a}_i\vec{a}_j$. ^b Values refined for Ca_3SnH_2 .

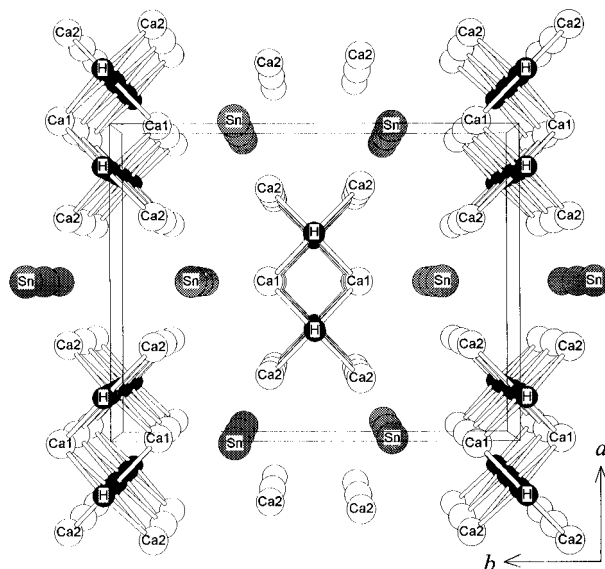
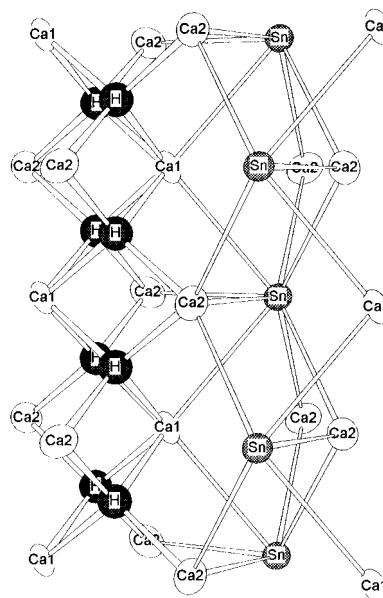
Table 5. Important Bond Distances and the Shortest [Ca–Ca] and [H–H] distances (\AA) in Ca_3TtH_2 (Tt = Sn, Pb)

atom–atom	Ca_3SnH_2	Ca_3PbH_2
H–Ca1 (2 \times)	2.24(2)	2.26
H–Ca2 (2 \times)	2.25(2)	2.26
Tt–Ca1 (2 \times)	3.4359(8)	3.468(2)
Tt–Ca2 (4 \times)	3.2987(7)	3.324(1)
Tt–Ca2 (2 \times)	3.453(1)	3.478(2)
Ca1–H (4 \times)	2.24(2)	2.26
Ca1–Tt (2 \times)	3.4359(8)	3.468(2)
Ca2–H (2 \times)	2.25(2)	2.26
Ca2–Tt (2 \times)	3.2987(7)	3.324(1)
Ca2–Tt (1 \times)	3.453(1)	3.478(2)
H–H	2.6100(5)	2.63
Ca1–Ca1	3.623(2)	3.641(3)
Ca1–Ca2 ^a	3.634(1)	3.672(3)
Ca2–Ca2	3.583(2)	3.621(4)

^a In-plane separation.

**Figure 2.** $\sim[100]$ view of the layered structure of Ca_3SnH_2 with hcp-like layers stacking normal to \bar{c} and hydrogen in tetrahedral interstices.

in Table 5. These, Yb_3SnH_2 and Yb_3PbH_2 are members of a new structure type as both Zintl phases and ternary metal hydrides. As shown by the $[100]$ view in Figure 2, the parent structure Ca_3SnH_2 is made up of layers of mixed Sn and Ca atoms. These are ordered and stacked hcp normal to \bar{c} such that hydrogen atoms lie in all nominally tetrahedral voids formed by Ca atoms and so generate chains of tetrahedra along \bar{c} that share Ca1, Ca2 edges. (Ca1 and Sn lie on sites of mm symmetry while Ca2 has m , and H, 2 symmetry.) In addition, pairs of these H-centered Ca_4H tetrahedral chains share Ca1–Ca1 edges in the a direction, Figure 3, to produce double chains of

**Figure 3.** View down $[001]$ of the structure of Ca_3SnH_2 to show the double calcium hydride chains surrounded by isolated Sn anions. A 2-fold axis through H lies vertical.**Figure 4.** Ca environments of H and Sn atoms in Ca_3SnH_2 (Ca, open, Sn, gray, and H, black, ellipsoids at 99% probability levels).

tetrahedra along \bar{c} that are separated by isolated Sn atoms. The center of Figure 4 shows how the Sn atoms (anions) are surrounded by eight Ca atoms in a distorted bicapped trigonal prism, with no hydrogen neighbors. These Sn-centered polyhedra share faces in the \bar{c} direction and are connected to H-centered tetrahedra by edge-sharing through calcium. A 2-fold axis parallel to \bar{a} that runs through the hydrogen pairs describes the stacking of adjacent layers, Figures 2 and 4. The structural details of these layers and their packing will be described later in connection with an analysis of the relationship of this structure to perovskite examples.

Another interesting feature of the Ca_3SnH_2 structure is the environments of the two Ca atoms, Figure 4. The Ca1 is bound to both four H atoms within the hydride chain that define a rectangle and to two tin atoms between the chains, while each Ca2 has two H neighbors within the chain and three Sn atoms between the chains.

The four effectively equal Ca–H bond distances in Ca_3SnH_2 , two each at 2.24(2) and 2.25(2) \AA (and 2.26 \AA in Ca_3PbH_2

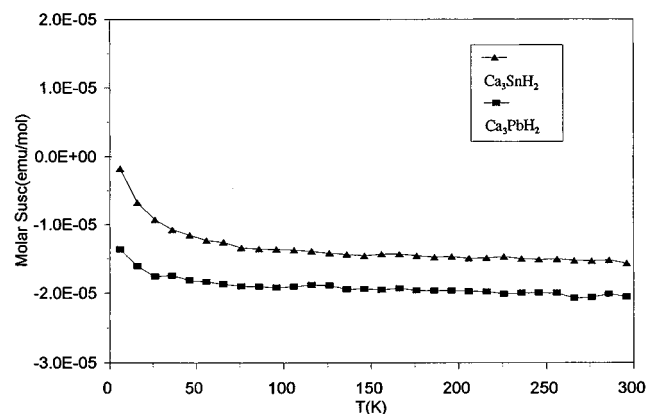


Figure 5. Temperature dependencies of the molar magnetic susceptibilities (χ_M) of Ca_3SnH_2 and Ca_3PbH_2 at 3 T.

without hydrogen refinement), are very consistent with both the sum of crystal radii of Ca^{2+} (1.14 Å¹⁹) and H^- (1.10 Å²⁰) and the average Ca–D distance in $\text{Ca}_5\text{Bi}_3\text{D}$ ($\text{Ca}_5\text{Sb}_3\text{F}$ -type), 2.26 Å.⁹ Bond valence calculations were performed around the hydrogen site using bond length parameters derived by Bressi and O’Keeffe²¹ from a limited number of hydrides. These gave Ca–H bond orders of 0.33 (Ca1) and 0.31 (Ca2) and bond order sums about H of 1.32 and 1.24 for Ca_3SnH_2 and Ca_3PbH_2 , respectively, close to the expected value of unity. (The size of hydride is known to depend significantly on the counterion size and charge.²²) The average Sn–Ca and Pb–Ca distances of 3.37 and 3.40 Å (CN8) are quite comparable to those estimated about the nine-coordinate Tt in the binary (Co_2Si -type) compounds Ca_2Sn , 3.36 Å, and Ca_2Pb , 3.40 Å, from powder data¹⁸ when a pair of longer (~3.7 Å) distances are included in the latter.

Properties. An oxidation state count for Ca_3TtH_2 indicates these are structurally Zintl phases, i.e., $3 \times 2 (\text{Ca}^{+2}) - 4 (\text{Tt}^{-4}) - 2 \times 1 (\text{H}^-) = 0$. The electronic conduction and magnetic properties of Ca_3SnH_2 and Ca_3PbH_2 are all consistent with this assignment. The expected semiconducting behavior of both was confirmed by “Q” measurements, which gave resistivities at room temperature of about 3 mΩ·cm with negative temperature coefficients for both. Both compounds are diamagnetic, as illustrated in Figure 5. The Ca_3SnH_2 phase has a χ_M value of about -1.5×10^{-5} emu/mol over about 100–300 K after correction for core contributions (-4.2×10^{-5} emu/mol). The Ca_3PbH_2 as synthesized exhibited a weakly positive susceptibility of $+5.0 \times 10^{-6}$ emu/mol over a 100–300 K range after core correction (-5.1×10^{-5} emu/mol). A temperature-independent impurity contribution ($\sim 2.5 \times 10^{-5}$ emu/mol) was estimated from the zero field intercept of M vs H data at 100 and 300 K, and correction for this left the sample diamagnetic (-2.0×10^{-5} emu/mol). The Yb_3TtH_2 isotypes presumably contain Yb(II) and have comparable properties.

Structural Comparisons. Some interesting relationships between the structure of the new Ca_3TtH_2 and those for related phases can be found. First, Ca_3Zn has a Re_3B -type structure with the same space group, Cmcm , but the 8-fold Ca set is now situated in an $8f$ (0, y , z) site,²³ and this generates a related structure with layers normal to \vec{a} but with the calcium atoms farther apart. Notwithstanding, the zinc is again found in a bicapped trigonal prism of calcium atoms. Comparison of the

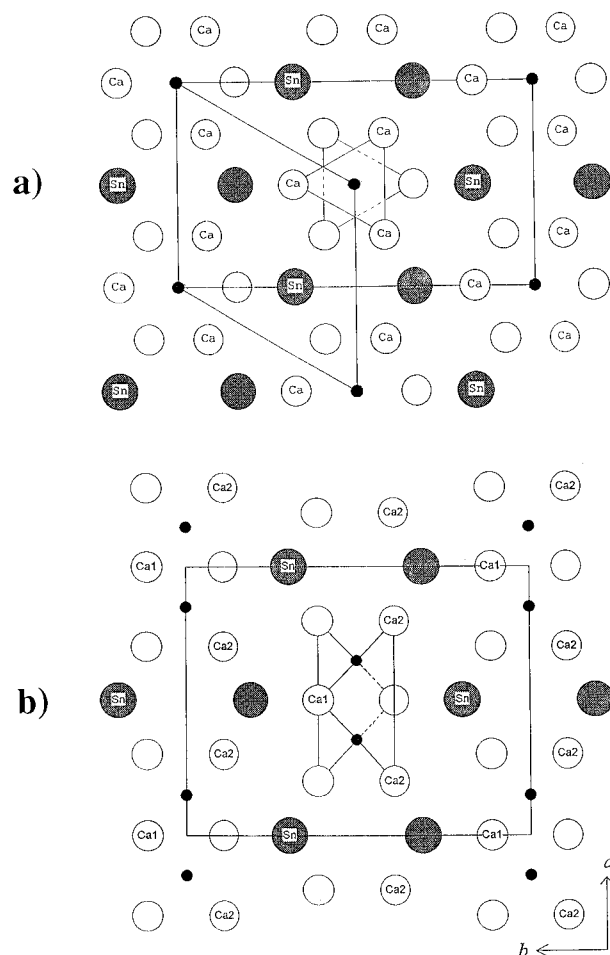


Figure 6. [001] view of (a) hexagonal Ca_3SnO (inverse perovskite) and (b) Ca_3SnH_2 on the same scale. Lettering or not distinguishes the bilayers, which are related by vertical 2 and 2_1 axes. The equivalent C-centered supercell is also outlined in the top view. The transition from (a) to (b) is accomplished by horizontal compression of the trigonal antiprismatic Ca_6O chains to yield the observed double chains of edge-sharing tetrahedra.

two compounds is of note since they would be analogous were Ca_3Zn to be formulated with an improbable $4s^2 4p^6$ closed-shell Zn^{-6} .

More comparable isoelectronic Zintl phases, ones that in fact prompted the present study, are the familiar Ca_3SnO and its analogues. These crystallize in a cubic antiperovskite type structure ($\text{Pm}\bar{3}m$).¹² The structure contains the customary mixed layers of composition Ca_3Sn ordered and stacked ccp so that O occupies all octahedral voids defined by only Ca atoms. Thus Ca_3SnH_2 differs from Ca_3SnO , and other isotypes, by the doubled number of nonmetal anions that need to be accommodated and, as usual, in tetrahedra rather than octahedral Ca environments, avoiding in both cases Sn^{4-} neighbors. There are no Ca_4 tetrahedral sites in the cubic Ca_3Sn substructure, only unsuitable Ca_3Sn types. But a very close analogue of the new structure can be found in the inverse version of the hexagonal perovskite structure of BaNiO_3 ($\text{P6}_3/\text{mmc}$)²⁴ in which single interstitial sites (Ni) would be centered within confacial trigonal antiprismatic chains of calcium (O) atoms with tin (Ba) atoms between them. One then needs only a way to split the single octahedral sites into pairs of tetrahedral cavities. To do so, the parent $\text{P6}_3/\text{mmc}$ structure needs to distort into one with the observed maximal non-isomorphic subgroup Cmcm . The

(19) Shannon, R. D. *Acta Crystallogr.* **1976**, A32, 751.

(20) Marek, H. S.; Corbett, J. D. *Inorg. Chem.* **1983**, 22, 3194.

(21) Bressi, N. E.; O’Keeffe, M. *Acta Crystallogr.* **1991**, B47, 192.

(22) Bronger, W. Z. *Anorg. Allg. Chem.* **1996**, 622, 9.

(23) Fornasini, M. L.; Merlo, F. *J. Less-Common Met.* **1981**, 79, 111.

(24) Takeda, Y.; Kanamaru, F.; Shimada, M.; Koizumi, M. *Acta Crystallogr.* **1976**, B32, 2464.

process is shown in Figure 6 for (a) hexagonal Ca_3SnO and (b) orthorhombic Ca_3SnH_2 , where the atom lettering or not distinguishes the two layers. (Vertical 2-fold rotation and 2_1 screw axes are the most useful symmetry operations.) As can be seen in the figure, the hydride structure (b) is generated directly from that of the perovskitic Ca_3SnO (a) by radial (horizontal) compression of the trigonal antiprismatic chains until the diagonal Ca–Ca distances across the antiprisms equal the interplanar separation, which process generates a pair of Ca tetrahedra sharing Ca1–Ca2 edges. This means the basal faces of the antiprisms need to be compressed into isosceles triangles. A pair of the “before and after” polyhedra are outlined in the center of the respective parts of Figure 6. The largest dimensional changes are a substantial expansion in a_{orth} as the two tetrahedra are “squeezed out”, which also causes puckering of what were horizontal Ca rows in the upper sketch. The $\text{Ca}_3\text{-Sn}$ nets in the hydride now have a topology with relatively low

symmetry, each containing distorted squares and two types of triangles in a 1:4 ratio which stack with Ca1 on the squares.

This distortion appears to be a remarkably direct means of doubling the interstitial count in a structural regime dominated by more-or-less close-packed Ca_3Sn layers. The principal symmetry losses are the 3-fold axes along which the Sn atoms lie in hexagonal Ca_3SnO . But there is little reason to believe the change could take place in a concerted manner.

Acknowledgment. We thank J. E. Ostenson for the magnetic measurements.

Supporting Information Available: More details on crystallographic studies of Ca_3SnH_2 and Ca_3PbH_2 and anisotropic displacement parameters are available in two CIF files. Access information is given on any current masthead page.

IC970289U